Voyage 2050 white paper

Unveiling the faint ultraviolet Universe

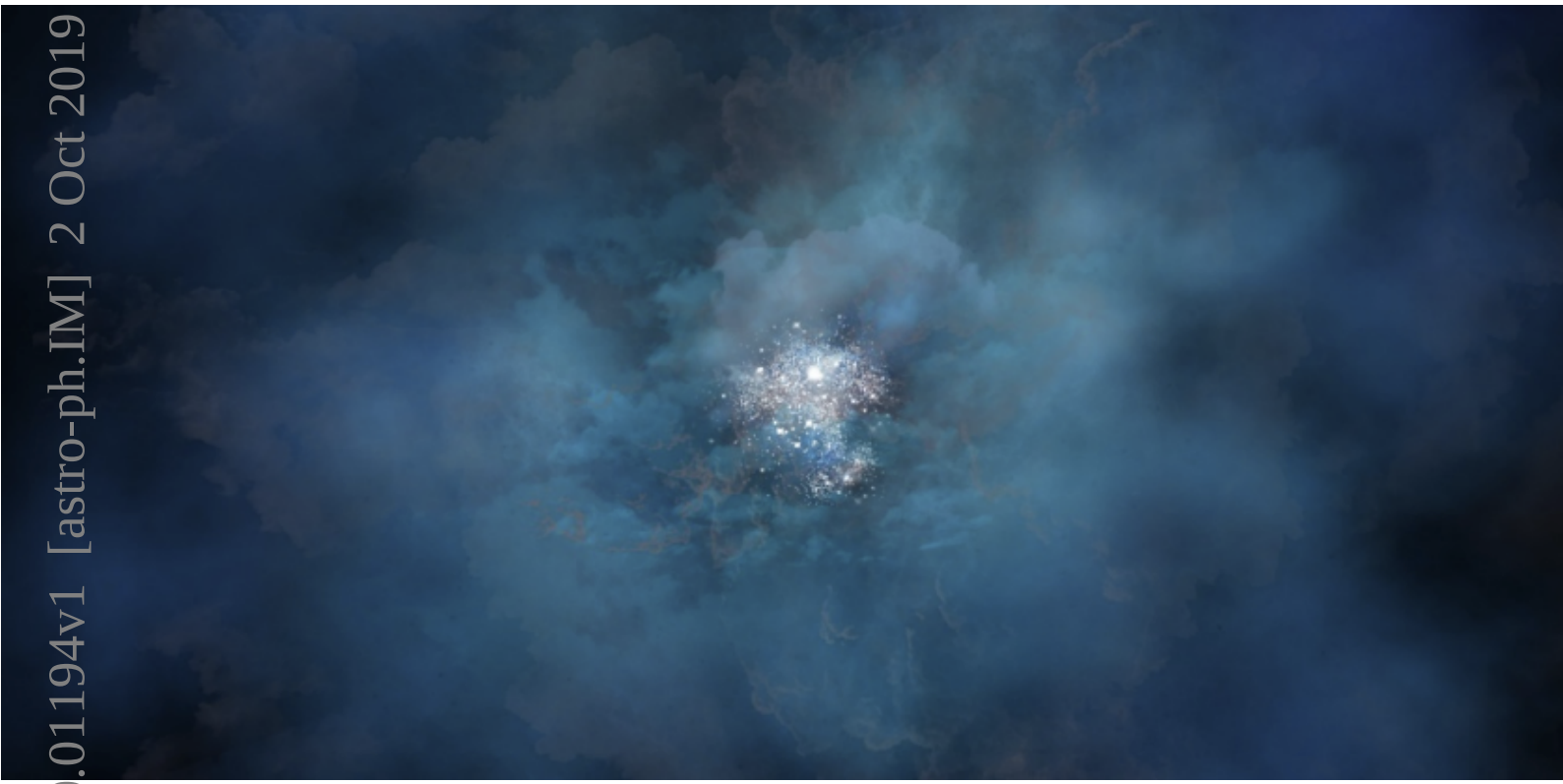

Contact scientist: Anita Zanella

European Southern Observatory
Karl-Schwarzschild-Str. 2, 85748 Garching bei München, Germany
Email: azanella@eso.org

Proposing team: A. Zanella[1], C. Zanoni[1], F. Arrigoni-Battaia[2], A. Rubin[1], A. Pala[1], C. Peroux[1], R. Augustin[1,3], C. Circosta[1], E. Emsellem[1], E. George[1], D. Milakovic[1], R. van der Burg[1]

[1]European Southern Observatory, Karl-Schwarzschild-Str 2, 85748 Garching bei München, Germany
[2]Max-Planck-Institut für Astrophysik (MPA), Garching bei München, Germany
[3]Aix Marseille Université, CNRS, LAM (Laboratoire d'Astrophysique de Marseille) UMR 7326, F-13388 Marseille, France

Acknowledgments: We are grateful to J. Kosmalski, J. Spyromilio, Chian-Chou Chen, F. Lelli, and T. Kupfer for useful discussions and inputs.

On the cover page: An artist's impression showing the gaseous halo surrounding a galaxy, illuminated by ultraviolet light called Lyman alpha emission. Credit: T. Klein, UWM.

1 Project overview

New and unique science opportunities in several different fields of astrophysics are offered by conducting spectroscopic studies of the Universe in the ultraviolet (UV), a wavelength regime that is not accessible from the ground. We present in the following some of the scientific challenges that can be addressed with a space-based mission in 2035 – 2050.

- By detecting the intergalactic medium in emission it will be possible to unveil the cosmic web, whose existence is predicted by current theories of structure formation, but it has not been probed yet. This will enable studies of the exchange of baryons between galaxies (and quasars) and their surroundings, unveiling how the halo gas contributes to the evolution of galaxies and what mechanisms drive the galaxy angular momentum build-up through cosmic time. Finally, multiple detections of the intergalactic medium in emission will provide measurements of the UV background, a critical quantity used in simulations of galaxy formation, still poorly constrained in observations (Section 2.1, 2.2).

- Observations of the neutral gas distribution (by mapping the Lyman-α emission) in low-redshift galaxy cluster members will clarify the efficiency with which ram-pressure stripping removes the gas from galaxies and the role of the environment in quenching star formation. These observations will be crucial to understand how and when the red sequence of galaxies is assembled in dense environments. These observations will be key in interpreting high redshift observations, where currently the Lyman-α is more easily accessible (Section 2.3).

- By observing statistical samples of supernovae in the UV it will be possible to characterize the progenitor population of core-collapse supernovae, providing the initial conditions for any forward-modeling simulation and allowing the community to progress in the understanding of the explosion mechanism of stars, as well as the final stages of stellar evolution (Section 2.4).

- Targeting populations of accreting white dwarfs in globular clusters it will be possible to constrain the evolution and fate of these stars and investigate the properties of the most compact systems with the shortest orbital periods which are expected to be the brightest low frequency gravitational wave sources. The possibility will also be explored that accreting white dwarfs are progenitors of Type Ia supernovae, which are fundamental sources to constrain cosmological distances and the existence of dark matter (Section 2.5).

A UV-optimized telescope (wavelength range $\lambda \sim 90$ - 350 nm), equipped with a panoramic integral field spectrograph with a large field of view (FoV $\sim 1 \times 1$ arcmin^2), with medium spectral (R = 4000) and spatial ($\sim$ 1" – 3") resolution will allow the community to simultaneously obtain spectral and photometric information of the targets, and tackle the science questions presented in this paper (Section 5). The data that result from this kind of observation will contain an enormous amount of information and hence will have a great legacy value for the whole scientific community. Additionally, these observations will open up completely new areas of

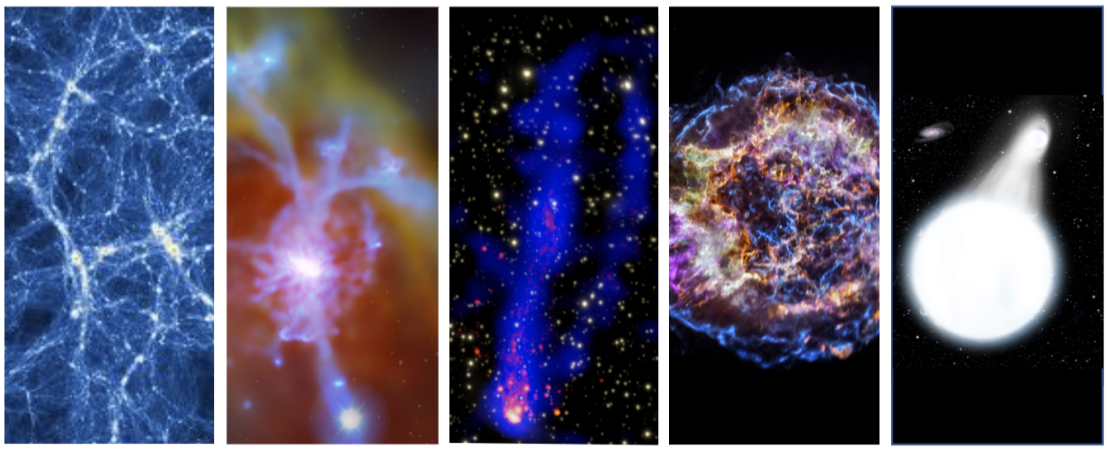

Figure 1: Artistic impression of the different science questions addressed by this proposal. From left to right: large scale structure (OWLS, Schaye et al. 2010); circumgalactic medium around galaxies (MPIA, credit: G. Stinson and A. V. Macció); gas stripping (credit: X-ray NASA/CXC/UVa/, H-alpha/Optical SOAR/MSU/NOAO/UNC/CNPq-Brazil); supernovae (credit: NASA/CXC/SAO); binary white dwarfs (credit: David A. Aguilar).

the parameter space, allowing the proposed mission to have a great potential for serendipitous discoveries.

In the coming years, when most of the new large facilities such as the Extremely Large Telescope (ELT) and the James Webb Space Telescope (*JWST*) will focus on the infrared (IR) wavelength range, and the Hubble Space Telescope (*HST*) will not be operational anymore, a mission in the UV with the capability of observing spectroscopically large areas of the sky will be unique. In synergy with the ELT instruments, Square Kilometer Array (SKA), and Atacama Large Millimeter Array (ALMA), but also with other space-based missions such as the Advanced Telescope for High Energy Astrophysics (*Athena*) and the Laser Interferometer Space Antenna (*LISA*) it will allow us to push further our current understanding of the Universe.

In the next Sections we will present the main science themes to be addressed in the coming decades (Figure 1, Section 2) and we will place them in the framework of the current and future technological development (Section 5). We will also discuss the uniqueness of the proposed straw-man mission and instrument (Section 3) and its synergies with future facilities (Section 4).

2 Science cases

2.1 Unveiling large-scale structures in emission at $z \lesssim 1.7$

The current paradigm of structure formation predicts the presence of gaseous filaments connecting galaxies (e.g., White et al. 1987, Bond et al. 1996), ultimately forming an intricated web known as intergalactic medium (IGM; Meiksin 2009). At present, the existence of the IGM is confirmed only indirectly by observations of the large scale structures traced with galaxy surveys at low redshift and by studies of the Lyman-α (Lyα) forest in absorption against background quasars. Obtaining direct images and properties of the cosmic web, and being able to study its evolution through cosmic history will represent a major breaktrough for cosmology. However, given the expected low densities for such gas ($n_{\rm H} \lesssim 0.01$ cm^{-2}) and the budget of ionizing photons in the ultraviolet background (UVB; e.g., Haardt & Madau 2012), its direct observation is predicted to be very challenging (surface brightness in Lyα predicted to be $\rm SB_{Ly\alpha} \sim 10^{-19} - 10^{-20}$ erg s^{-1} cm^{-2} arcsec^{-2}; Gould & Weinberg 1996; Bertone & Schaye 2012; Witstok et al. 2019). A direct detection of the IGM appears to be so far elusive even with top-notch current facilities on 10m class telescopes (e.g., Gallego et al. 2018; Wisotzki et al. 2018), e.g., the Multi Unit Spectroscopic Explorer (MUSE; Bacon et al. 2010) and the Keck Cosmic Web Imager (KCWI; Morrissey et al. 2012). Being based on Earth, these instruments can target the Lyα emission only above the atmospheric cut-off ($z \gtrsim 1.7$) and thus fight against a strong cosmological surface brightness dimming $(1+z)^{-4}$.

Astronomers have tried to bypass these limitations by searching the IGM signal around quasars. A quasar is expected to act as a flashlight, photoionizing the surrounding medium out to large distances. The ionized gas would then recombine, emitting as the main product Hydrogen Lyα photons in copious amounts (e.g. Rees 1988; Haiman & Rees 2001). The boosted Lyα glow ($\rm SB_{Ly\alpha} > 10^{-19}$ erg s^{-1} cm^{-2} arcsec^{-2}) should then possibly be at reach for state-of-the-art instruments (Cantalupo et al. 2005; Kollmeier et al. 2010).

Following this idea, several works used Lyα emission from halos to constrain the physical properties of the diffuse gas phases out to intergalactic scales around individual high-redshift quasars (Tumlinson et al. 2017, Hu & Cowie 1987; Heckman et al. 1991; Møller et al. 2000; Weidinger et al. 2004, 2005; Christensen et al. 2006; Cantalupo et al. 2014; Martin et al. 2014; Arrigoni Battaia et al. 2016; Farina et al. 2017). At $z \sim 3$, MUSE observations can now easily ($\sim$ 1 hour on source; surface brightness limit of $\rm SB_{Ly\alpha}^{1\ arcsec^2} \sim 10^{-18}$ erg s^{-1} cm^{-2} arcsec^{-2}) uncover the emission within 50 projected kpc from the targeted quasar and reaching out to distances of $\sim$ 80 projected kpc (Borisova et al. 2016; Arrigoni Battaia et al. 2019). However, it is evident that detections of diffuse emission at intergalactic distances ($>$ 100 kpc) at high z are favored when additional active companions are present in close proximity (Hennawi et al. 2015; Arrigoni Battaia et al. 2019, 2018), or much more sensitive observations are conducted ($>$ 10 hours). Scientific teams have started to change their approach in unveiling the IGM emission, passing from the targeting of individual quasars to (i) short (Cai et al. 2018) or extremely long integrations ($\gg$ 40 hours; Lusso et al. 2019) of multiple high-redshift quasars, or overdensities hosting quasars (Cai et al. 2017), and (ii) stacking of ultra deep observations of several galaxies (Gallego et al. 2018; Wisotzki et al. 2018). Therefore the detection of the gas emission on large scale still relies on the presence of quasars. Additionally, these studies show that most

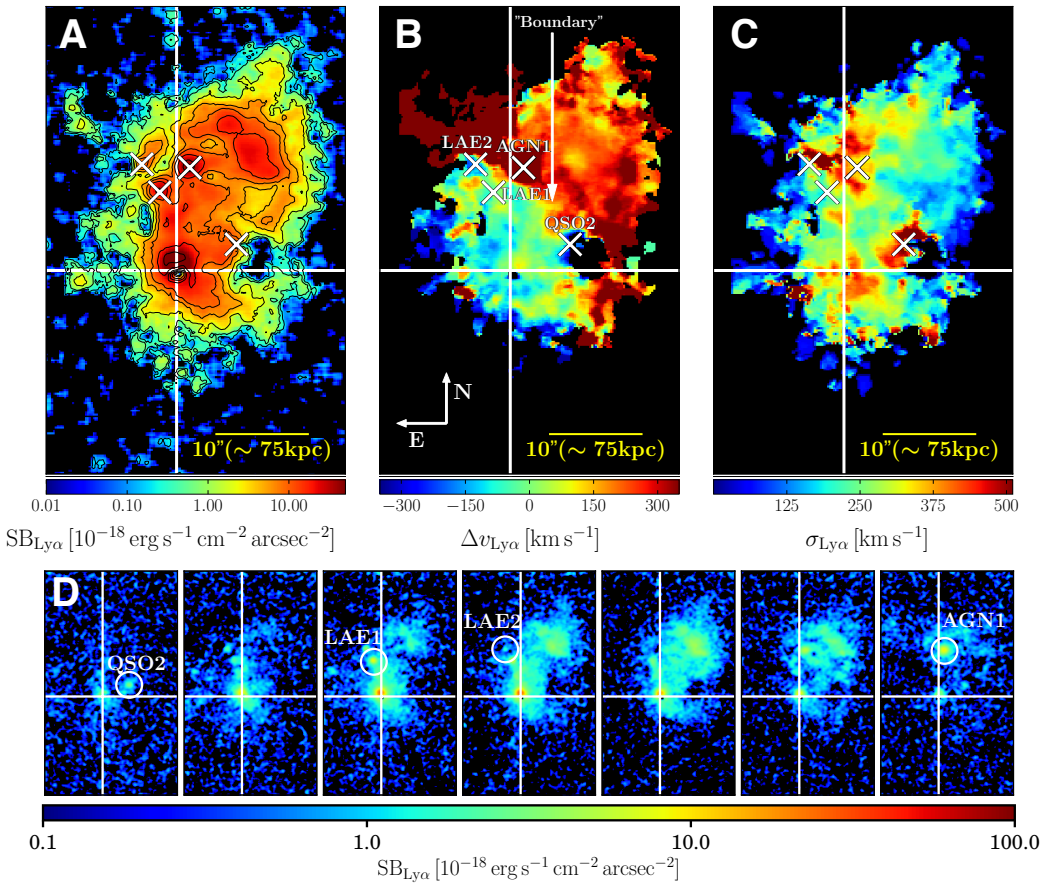

Figure 2: An example of current large-scale structures detected in Lyα around quasars with VLT/MUSE at high redshift: the enormous Lyα nebula around the $z = 3.164$ quasar SDSSJ 1020+1040 (Arrigoni Battaia et al. 2018). **(A)** "optimally-extracted" Lyα surface brightness map obtained after subtraction of the quasar point-spread-function and continuum . The black contours indicate the isophotes corresponding to a signal-to-noise ratio of S/N = 2, 4, 10, 20, 30, 50, and 100. This image reveals an extremely bright nebula (SB$_{Ly\alpha} \sim 10^{-17}$ erg s^{-1} cm^{-2} arcsec^{-2}) extending on the NW side of the quasar. Additional four strong Lyα emitters (diagonal crosses) are associated with the quasar, and the nebular emission. Two of these sources have been spectroscopically confirmed as AGN, making this system the third known quasar triplet at high z. **(B)** flux-weighted velocity-shift map with respect to the systemic redshift of the quasar obtained from the first-moment of the flux distribution. A velocity shear between the SE and NW portion of the nebula is evident. The transition region is referred to as the "Boundary". **(C)** velocity dispersion map obtained from the second-moment of the flux distribution. Regions of higher dispersion ($\sigma_{Ly\alpha} \approx 430$ km s^{-1}) are visible in proximity of the three AGN, but overall the Lyα nebula shows quiescent kinematics ($\sigma_v < 270$ km s^{-1}). **(D)** Each cut-out image (same size as A, B, and C) shows the surface brightness map of the ELAN within a 3.75 Å layer (3× MUSE sampling) in the wavelength range 5058 Å $\lesssim \lambda \lesssim$ 5084 Å (from left to right). In all of the panels (A, B, C, D) the large white cross indicates the position of the quasar prior to PSF subtraction. Figure adapted from Arrigoni Battaia et al. (2018). Currently, similar large-scale emission cannot be probed at low z ($z \lesssim 1.7$) because of the absence of dedicated facilities.

of the uncertainty in the search for the direct emission from IGM filaments at high z resides on the lack of well-known large-scale structures as traced by galaxies.

Notwithstanding the aforementioned difficulties, state of the art integral field unit (IFU) spectrographs instruments started to open new possibilities in the study of the gas distributed at large scales at high redshift, by pushing the sensitivity of observations to $SB_{Ly\alpha} \sim 10^{-19} - 10^{-20}$ erg s^{-1} cm^{-2} arcsec^{-2}. A new-generation space mission optmized for UV observations is needed to complement the ongoing efforts to study the large scale structure at high-z by opening an unexplored window at low-z. By routinely detecting the IGM in emission at $z \lesssim 1.7$, this instrument will allow us to achieve the following science goals:

- Connect the dots at low redshift: test our current view of the matter distribution at low z by detecting the cosmic web in emission (through rest-frame UV emission lines) surrounding galaxies and quasars. This is crucial as currently we have a good understanding of the distribution of large-scale structures as traced only by galaxies at low z.
- Directly study the properties (e.g., density, metallicity) of the IGM in emission, complementing the information acquired from studies of the Lyα forest.
- Thanks to multiple detection of the IGM in emission, provide measurements of the UV background at low z that do not rely on the statistics of the IGM in absorption. The UV background is a critical quantity used in all simulations and models of structure formation, but it is still poorly constrained observationally. Its precise determination is key for our understanding of galaxy formation and evolution.
- Study of the gas kinematics within large-scale structures surrounding galaxies, allowing a direct characterization of the galaxy angular momentum build-up through cosmic time.

2.1.1 The need for space-based UV observations

Recent works show that the most efficient and effective way to detect emission extending to hundreds of kpc scales around high-z quasars and galaxies is the use of wide-field IFU instruments (e.g., Figure 2; Arrigoni Battaia et al. 2018). Space-based, wide-field spectroscopic observations in the wavelength range $\lambda \sim 90 - 350$ nm will allow us to achieve our scientific goals. Specifically, a space-based instrument is needed to observe the Lyα transition at low z ($z \lesssim 1.7$), where the surface brightness dimming is less severe. Assuming similar properties for the gas, it will be possible to target sources with 16× lower surface brightness at $z \sim 0.5$ with respect to $z \sim 3$. Furthermore, a wide field of view (1×1 arcmin^2, which corresponds to hundreds of kpc at $z \lesssim 1.7$) is needed to both image at once large-scale structures and to survey large parts of the sky. As we are interested in detecting large scale structures with very low surface brightness, large pixels (e.g. ~ 1 arcsec) are preferred (as in e.g. KCWI; Morrissey et al. 2012).

2.2 Probing the Circum Galactic Medium around galaxies in emission

Understanding the complex mechanisms regulating galaxy formation is one of the main questions today in cosmology and astrophysics. The question of how galaxies gather gas to sustain

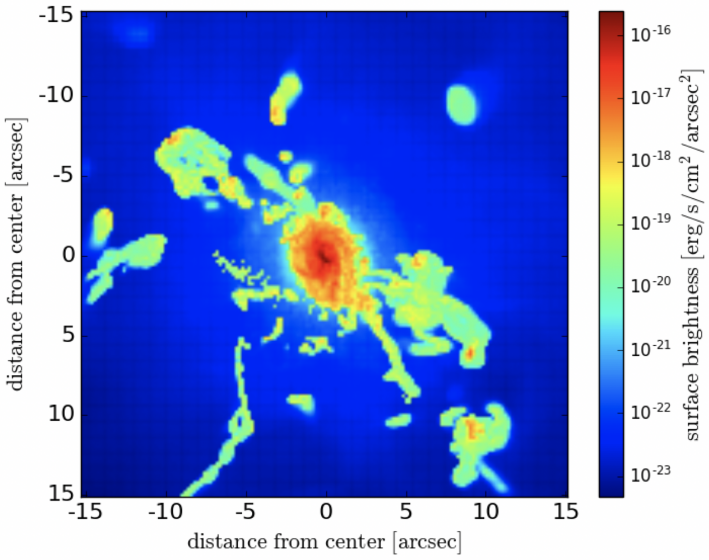

Figure 3: Example of a mock Lyα CGM halo around a $z = 0.7$ galaxy, from RAMSES cosmological simulations (Augustin et al., in prep). The Lyα line is at 206 nm and 1" $\sim$ 7 kpc at the redshift of this source. The CGM surface brightness levels shown in this map will be within reach of the proposed UV instrument.

star formation is of particular interest, as it can shed light on the fact that the star formation rate (SFR) has been declining from $z \sim 2$ while diffusely distributed hydrogen is still the dominant component for the total baryonic mass budget (as compared to hydrogen in stars, Madau & Dickinson 2014). The outflowing and accreting gas interacts around galaxies on scales up to hundreds of kpc (the Circum Galactic Medium, CGM). Studying the CGM is fundamental to understand the cosmic baryon cycle (Steidel et al. 2010, Shull et al. 2014, Tumlinson et al. 2017) and it will provide key constraints on the question of galaxy formation and evolution. Absorption spectroscopy has already shed light on the distribution and the chemical composition of the CGM gas, but only on a statistical point of view, given that only one line of sight per galaxy can be probed due to the scarcity of background quasars in the vicinity of galaxies (Noterdaeme et al. 2012, Pieri et al. 2014, Quiret et al. 2016, Rahmani et al. 2016, Krogager et al. 2017, Augustin et al. 2018). Yet, mapping the CGM in emission is the natural next step to fully understand it.

2.2.1 The need for space-based UV observations

The achieve the science goals presented above it is key to detect and map different lines (e.g. Lyα, CIV, OVI, CVI, OVIII) arising from the CGM of low-redshift galaxies. The signal (surface brightness) scales with $(1 + z)^{-4}$ so that lower redshift observations are considerably easier in turn requiring space-born UV facilities to measure rest-frame UV lines. IFU-like capabilities are key for obtaining maps and kinematic reconstructions of the gas in the halos of galaxies. A field of view of $\sim 1 \times 1$ arcmin^2 will cover most of the CGM region of a galaxy at $z \sim 1$. Modest

spatial resolution (to increase sensitivity) and spectral resolution (R $\sim$ 4000) are sufficient. Such program will be complementary to similar high-redshift projects making use of extrememly large ground-based telescopes (i.e. ELT/HARMONI). An example of mock Lyα CGM halo at $z = 0.7$ from dedicated RAMSES cosmological hydrodynamical simulations is shown in Figure 3 (Augustin et al., in prep).

2.3 Ram-pressure stripping and quenching in galaxy clusters

The existence of a well defined separation among massive, red, early-type, quiescent galaxies and blue, late-type, actively star-forming objects is fundamental for the current modeling of galaxy formation and evolution. Nowadays, "normal" galaxies are thought to assemble their mass through a secular process of star formation in a relatively steady state, forming a "Main Sequence" up to high redshift (e.g. Daddi et al. 2007, Speagle et al. 2014) and following a tight gas-star formation rate (SFR) density relation ("KS" relation, Schmidt 1959, Kennicutt 1998). Deviations from this dynamic equilibrium may occur in short starbursting events (typically associated with major mergers, Sanders & Mirabel 1996) or due to the cessation of star formation ("quenching"). Both these deviations from equilibrium are poorly understood: why do galaxies suddenly ignite the formation of thousands of stars per year? Why do they stop forming stars? The deviations from the Main Sequence and the KS relation might be connected: the merger of gas-rich objects may first result in a burst of star formation, followed by a drop of SFR and the subsequent quenching of the galaxy. The results of this process might be the compact, quiescent galaxies observed at $z \lesssim 2$ (e.g. Cimatti et al. 2008, Toft et al. 2014). However, it is still debated what is the mechanism responsible for stopping star formation and how galaxies are maintained quiescent for several Gyrs.

An additional piece of the puzzle is the correlation between galaxy colour and morphology with both local environment and stellar mass (Dressler 1980, Bell et al. 2004, Peng et al. 2010). The dependence on the environment seems to indicate that not only internal, but also external physical processes play a role in shaping the star formation of galaxies at all cosmic ages (Boselli et al. 2006, Blanton & Moustakas 2009). Internal mechanisms such as feedback from supernovae and active galactic nuclei (AGN, e.g. Hopkins et al. (2012), Croton et al. 2006), dynamical stabilization (Martig et al. 2009), and gravitational heating (Johansson et al., 2009) are deemed responsible for suppressing and quenching star formation at all densities. Environmental processes in the form of ram pressure or viscous stripping, tidal interactions (Gunn & Gott, 1972), and the consumption of the galaxy's gas reservoir by star formation without further replenishment from the cosmic web because of accumulation of hot plasma inducing shocks and heating up infalling gas (e.g. Larson et al. 1980, Peng et al. 2015; Dekel & Birnboim 2006) seem to be key players in shaping the observed colour bimodality within galaxy clusters and groups, especially at the faint end of the galaxy luminosity function.

In the local Universe, the smoking gun of the role of ram pressure stripping in quenching star formation is the disturbed gas content of galaxy cluster members. Radio surveys at 21 cm revealed the HI deficiency of spiral galaxies in overdense environments, especially in the vicinity of the cluster core (Haynes 1985) and more recently the molecular gas deficiency has also been reported (Fumagalli et al. 2009, Boselli & Gavazzi 2014). Furthermore, these galaxies often

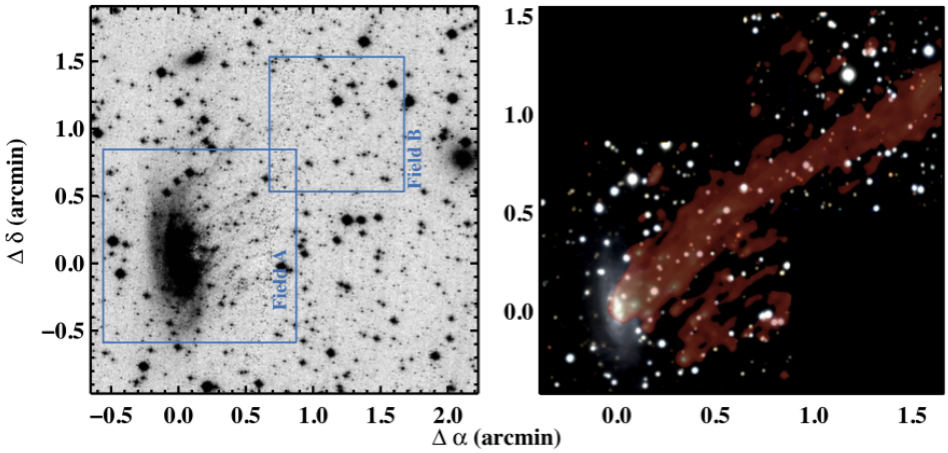

Figure 4: Example of a local cluster member undergoing ram pressure stripping observed with VLT/MUSE: ESO137-001 at $z = 0.016$ (Fumagalli et al., 2014). **Left**: HST/ACS image in the F475W filter with, superposed, the MUSE field of view at the two locations targeted by the observations. **Right**: RGB colour image obtained combining images extracted from the MUSE data cube in three wavelength intervals ($\lambda = 500 - 600$ nm for the B channel, $\lambda = 600 - 700$ nm for the G channel, and $\lambda = 700 - 800$ nm for the R channel). A map of the Hα flux is overlaid in red using a logarithmic scale, revealing the extended gas tail that originates from the high-velocity encounter of ESO137-001 with the intra-cluster medium.

show disturbed gas morphologies and tails visible both in Hα (Figure 4) and UV continuum (e.g. Gavazzi & Jaffe 1985, Fumagalli et al. 2014, Fossati et al. 2016).

At high redshift ($z \sim 1 - 1.5$) instead there is still no consensus on the influence of the environment on galaxies' gas content (Aravena et al. 2012, Dannerbauer et al. 2017, Coogan et al. 2018). This is mainly driven by the lack of detections that are generally limited to the most gas-rich members. Galaxies undergoing ram pressure stripping are ideal laboratories to constrain the efficiency with which gas can be removed and star formation is quenched. Observations of galaxy clusters and groups at different redshifts are therefore key to understand how and when the red sequence of galaxies is assembled in dense environments.

2.3.1 The need for space-based UV observations

To study quenching mechanisms in dense environments and the origin of galaxies' red sequence a space-based instrument with a large field of view ($\sim 1 \times 1$ arcmin^2), exquisite sensitivity, and a spectral coverage $\lambda \sim 90 - 350$ nm. This part of the spectrum includes the Lyα emission line at redshift $z \lesssim 1.7$. Lyα traces the neutral gas, which is expected to be the bulk of the material stripped by ram pressure, and is expected to be $> 10\times$ brighter than Hα (e.g. Scarlata et al. 2009). Mapping the Lyα emission with a wide-field spectrograph will allow us to trace stripped gas out to large distances from the galaxy (~ 500 kpc at $z = 1$) and to unveil gas tidal tails $\gtrsim 10\times$ fainter than the Hα ones, therefore targeting also the less massive cluster memebers. The detection of other emission lines (e.g. CIII, OI, HeII, MgII) will allow us to constrain the

density, temperature, and metallicity of the ionized gas. The comparison of the Lyα and Hα fluxes will also give information about the powering mechanisms of Lyα (e.g. shocks, star-formation, cooling), still an unknown issue. The spectral resolution of R $\sim$ 4000 will allow us to probe the kinematics of both the gas and stellar components to understand whether cluster members are mainly fast rotators, as expected if their star formation has been quenched after the interaction with the hot intra-cluster medium, or rather whether their gas has been stripped by more violent interactions with other cluster members (Toloba et al., 2011). These observations will be key to obtain the first detections of neutral gas stripping in $z \sim 1 - 1.5$ galaxy clusters, bridging the local and high-redshift Universe and understanding when and how galaxies become quiescent.

The stripped gas is expected to be mainly in the cold atomic phase, but it could be heated and change phase once it interacts with the hot gas confined withing the potential well of the cluster. Complementary multifrequency observations will allow us to reach a comprehensive picture of these phenomena: SKA will allow us to observe the cold HI gas at 21 cm, the molecular phase is detectable through CO (ALMA), and the hot gas phase is visible in the X-rays (*Athena*). Finally, ELT instruments will allow us to detect the ionised gas component.

2.4 Supernovae

Core collapse supernovae are the most common form of stellar death (Li et al., 2011). These events are the end-stage of massive stellar evolution, and are responsible for the chemical enrichment of the galaxy. While many supernovae have been discovered and observed, the characteristics of the stars that explode are still a mystery. Observationally it has been established that massive stars ($> 8M_{\odot}$) end their lives as a core-collapse supernova. However, theoretical models have not succeeded in reproducing the observed explosion properties, and more importantly cannot self-consistently explode the star without an artificial ignition (Burrows, 2013). The progenitors of core-collapse supernovae have been positively identified for a handful of events (Smartt et al., 2009; Smartt, 2015). The progenitor's characteristics are one of the major open questions which must be addressed in order to progress our understanding of the explosion mechanism of stars, as well as the final stages of stellar evolution.

The most robust technique for identifying progenitors is with high-resolution images taken from before the explosion. This technique has been successfully employed a handful of times using primarily *HST* images taken before the events (Smartt et al., 2004; Maund et al., 2011; Van Dyk, 2017). Some core-collapse supernovae seem to originate from red supergaint stars, but there is also an example of a Type IIb originating from a yellow hypergiant (Maund et al., 2011; Bersten et al., 2012). Two limitations prevent this technique from significantly advancing the field in the future: first, an image of the location from before the explosion is needed; second, it is necessary to wait for $5 - 10$ years until the supernova fades to below the progenitors' luminosity in order to confirm that the star terminally exploded and disappeared. Even when the second criterion is satisfied, some doubt remains as the star could be enshrouded in a high-extinction dust. Given these limitations, pre-explosion imaging is unlikely to increase the number of identified progenitors by orders of magnitude in the future.

The solution is to use semi-analytic models which have been developed in recent years (Waxman et al., 2007; Nakar & Sari, 2010; Rabinak & Waxman, 2011; Sapir & Waxman, 2017).

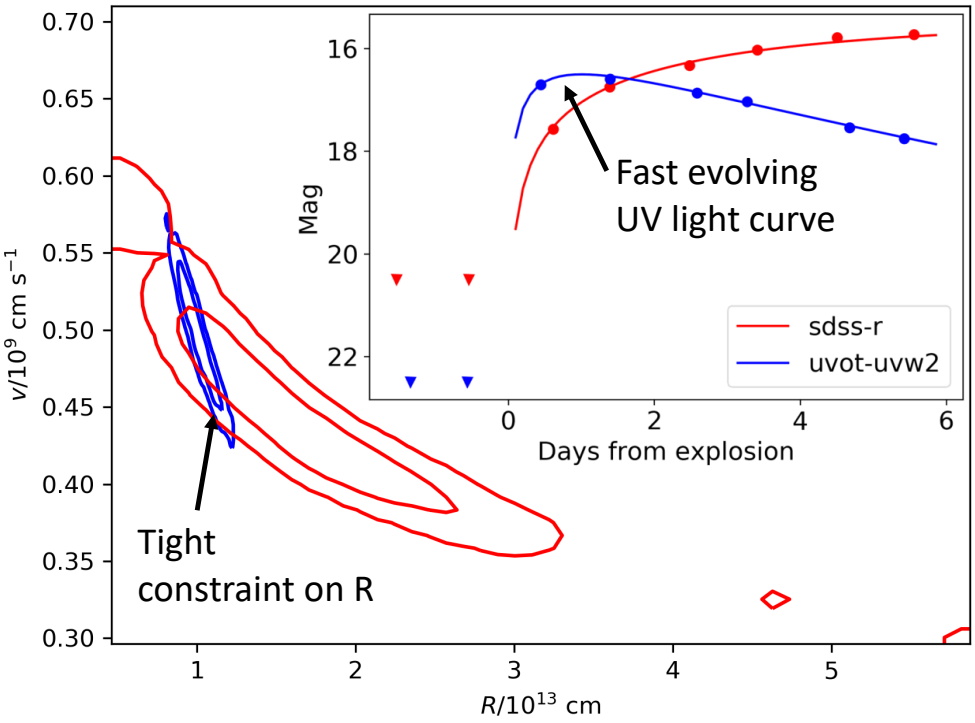

Figure 5: Constraints on radius and ejecta velocity (energy per unit mass of the explosion). In the inset we show a simulated light-curve as it would appear in UVOT-UVW2 and SDSS-r. The simulation is of an $R = 10^{13}$ cm progenitor observed with $\sim$ 1 day cadence. Note the faster rise of the UV light-curve. The contours represent 68% and 95% of the probability of the fit to the UV and visual bands separately. The UV is clearly more sensitive to the progenitor's radius than visual bands.

These models can relate the observed light curve of a core-collapse supernova to the progenitor's radius and the velocity of the ejecta (energy per unit mass of the explosion). These models can be applied to light curves of events which do not have pre-explosion images, and therefore have the potential to increase by orders of magnitude the number of identified progenitors. The hot ejecta ($> 10^4$ K) cools rapidly during the first days after the explosion. Because in the UV and optical wavelengths the blackbody spectrum is in the Rayleigh-Jeans regime, the UV light-curve evolves more rapidly than longer optical wavelengths (e.g. R-band). Shock-cooling models can only be applied to data taken during the first few days after explosions, therefore the rapid evolution of the UV light curve is critical for constraining the progenitor's properties. Rubin & Gal-Yam (2017) showed that visual-band wavelengths cannot constrain the progenitor's radius meaningfully, but that UV coverage at moderate (0.5 – 1 day cadence) can constrain the progenitor's radius to 20%. With a significant number of supernovae observed in the UV, it will be possible to measure the progenitor population of core-collapse supernovae. These will provide the initial conditions for any forward-modeling simulation that will be performed, and will provide benchmarks against which to design and test these simulations.

UV spectroscopy will also play a major role in understanding the composition of the progen-

itors. It has been shown that many supernovae have a circumstellar material surrounding the star from before the explosion (Gal-Yam et al., 2014; Yaron et al., 2017; Khazov et al., 2016). At the moment of first light, this material becomes highly ionized by the tremendous luminosity and temperature of the first photons of the explosions. After a timescale of hours to days the bulk of the supernovae ejecta sweeps up this material. During this window strong, highly ionized emission lines have been observed (e.g. OIII, HeII). These can be related back to the surface composition of the progenitor star in the last period before it exploded. Groh (2014) showed that the most informative lines are in the UV, e.g. CIV λ1548 – 1551, HeII λ1640, and NVI λ1718.

2.4.1 The need for space-based UV observations

To achieve our science goals we will need photometry of magnitude 20 sources with a cadence of 0.5 – 1 day. By simultaneously obtaining the spectra of our targets (with magnitude down to 20) with a signal-to-noise 10 we will measure the temporal evolution of the UV flux, and the strength and equivalent widths of the transient emission lines CIV λ1548 – 1551, HeII λ1640, and NVI λ1718, to achieve the science goals mentioned above (Figure 5).

2.5 Accreting white dwarfs in globular clusters: testing the models of compact binary evolution

Accreting white dwarfs (WDs), namely binaries in which a WD accretes from a main sequence star or a degenerate companion, are a strategical tool to probe the physical properties of the Universe and to test fundamental physical theories. The thermonuclear ignition of WDs following the interaction with a binary companion results in Type Ia supernovae (SNe Ia), which are fundamental yardsticks to constrain cosmological distance scales (Branch & Tammann, 1992) and the existence of dark energy (Riess et al., 1998; Perlmutter et al., 1999). Moreover, the most compact systems with orbital periods below one hour are among the brightest known low frequency gravitational wave sources and will be used to verify the performance of the space-based gravitational wave mission *LISA* and to calibrate the detector for future gravitational wave source discoveries (Kupfer et al., 2018). It is therefore critical to understand the evolution and final fate of accreting WDs.

Currently there are several significant discrepancies between the predictions of population synthesis models and the observed properties of accreting WDs. In particular (i) the interplay between the angular momentum loss mechanisms driving the evolution of accreting WDs at different orbital period regimes is poorly understood, (ii) the evolutionary path followed by the most compact systems is unknown, (iii) the final fate of accreting WDs and the pathway leading to SNe Ia explosions is still not clear. In particular (i) the interplay between the angular momentum loss mechanisms driving the evolution of accreting WDs at different orbital period regimes is poorly understood, (ii) the evolutionary path followed by the most compact systems is unknown, (iii) the final fate of accreting WDs and the pathway leading to SNe Ia explosions is still not clear. Solving these discrepancies is essential before the theoretical models can be sensibly applied to black hole and neutron star binaries, X-ray transients, and SN Ia progenitors.

Accreting WDs are predicted to be numerous in globular clusters ($\simeq$ 100 – 200 per cluster, Ivanova et al. 2006; Knigge 2012). Globular clusters (GCs) are therefore a unique laboratory

where to carry out statistical binary population synthesis studies for populations of accreting WDs with known distance, metallicity and age (Knigge (2012)). By observing populations of accreting WDs in GCs we will achieve the following goals.

- Constrain the evolution of accreting WDs. To test the prediction of the current models, measurements of the angular momentum loss rates at different orbital periods ($P_{\rm orb}$) are needed. However, the long timescales over which the orbital period changes typically prevent to obtain direct measurements. A proxy for the mean mass accretion rate and in turn for the angular momentum loss rate is the WD effective temperature ($T_{\rm eff}$, Townsley & Bildsten (2003); Bildsten et al. (2006)), as it is determined by compressional heating of the accreted material (Sion, 1995; Townsley & Bildsten, 2004). While several thousands accreting WDs are known, accurate temperatures are only measured for $\simeq$ 80 systems, obtained from ultraviolet *HST* observations (Bildsten et al., 2006; Townsley & Gänsicke, 2009; Pala et al., 2017). In this sample, only systems with a period 70 min $< P_{\rm orb} <$ 150 min show an angular momentum loss in agreement with model predictions, while all the others show discrepancies of more than one order on magnitude with the theory (Fig. 1).

- The formation of the most compact systems. Two main populations of accreting WDs are known: (1) the systems with main-sequence and brown-dwarf donors (cataclysmic variables, CVs) with orbital periods in the range 60 min $\lesssim P_{\rm orb} \lesssim$ 2 d and (2) the systems with helium stars or helium-core WDs as donors (AM CVn stars) with orbital periods $P_{\rm orb} \lesssim$ 60 min. The formation of AM CVn stars is still poorly understood and evolutionary models currently predict different formation scenarios (Nelemans et al., 2010). To observationally constrain different models it is key to study the chemical composition (e.g. N/O and N/C ratios) of the donor (Nelemans et al., 2010).

- Accreting WDs and SN Ia progenitors. Both CVs and AM CVns are intimately connected to the formation of SNe Ia. In fact, CVs with nuclear evolved donors undergo a phase of stable hydrogen shell burning during which the WD mass grow (possibly to the Chandrasekhar limit) and AM CVns accrete He-rich material from their degenerate donors, potentially triggering a SN Ia via the double-detonation mechanism (Bildsten et al., 2007; Fink et al., 2010). Determining the masses of these systems through a fit of the UV spectrum provides firm statistical constraints for the above scenarios and could finally confirm the potential of these systems as SN Ia progenitors. Also the rotation rates of accreting WDs are a critical parameter in the pathway leading to SNe Ia explosion. Absorption features from the photosphere of the WD accretor, which are only cleanly detected in the UV, can be used to measure the rotational velocity and determine whether the WD is spun up by accretion, allowing the WD to exceed the Chandrasekhar limit without triggering the SN explosion.

2.5.1 The need for space-based UV observations

The population of accreting WDs in GCs provides a statistically significant sample of systems spanning the whole orbital period distribution and will allow us to carry out stringent tests for

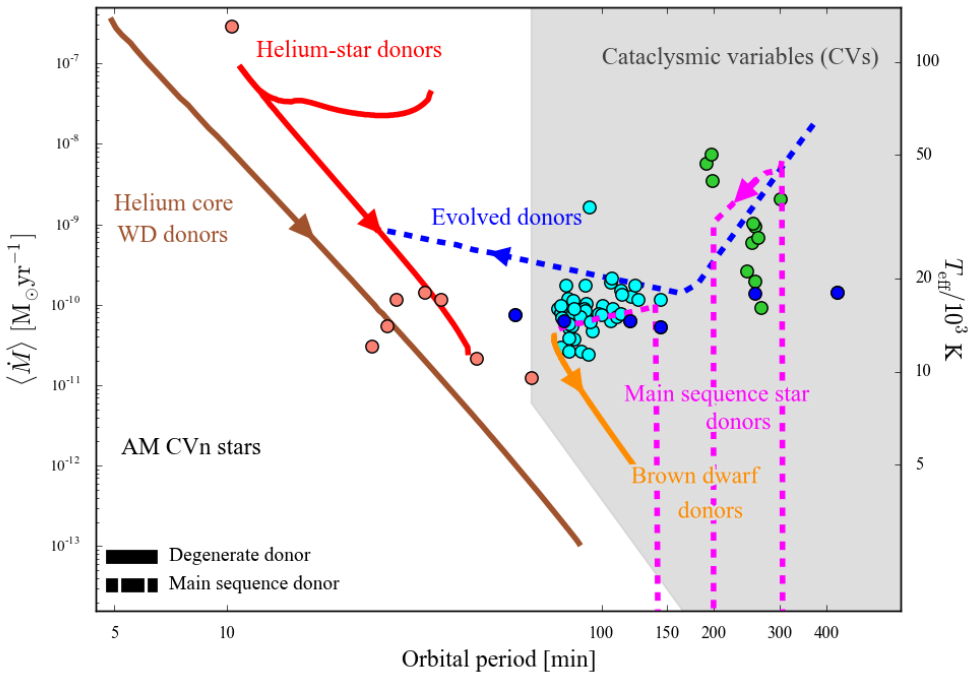

Figure 6: Effective temperatures of short-period (cyan) and long-period (green) CV WDs, AM CVns (pink) and systems with evolved donors (blue) (Bildsten et al., 2006; Townsley & Gänsicke, 2009; Pala et al., 2017). While the observations of short-period CVs (cyan) agree reasonably well with the theoretical evolutionary tracks, long-period CVs (green), AM CVns (pink) and systems with evolved donors (blue) are poorly studied and the few systems observed uncover major discrepancies between observations and models.

the current models of compact binary evolution. An IFU is required to deblend the sources in the dense environment of a GC (e.g. Husser et al. (2016)). Accreting WDs have typical temperatures $T_{\rm eff} \gtrsim 10\,000$ K and their spectral energy distribution peaks in the ultraviolet. In other wavelength domains, the emission is dominated by the disc (in the optical) or a boundary layer at the WD surface (in the X-rays). Space-based ultraviolet spectroscopy is therefore the only method to access and fully characterize the physical properties of these stars (e.g Szkody et al., 2002; Gänsicke et al., 2006; Sion et al., 2008; Pala et al., 2017). From the knowledge of the GC distance, the WD $T_{\rm eff}$ can be measured via a spectral fit to the ultraviolet data with synthetic atmosphere models thus providing a direct measurement of the angular momentum loss rate in the system (Townsley & Gänsicke, 2009). The spectral fit to ultraviolet data also provides the WD photospheric abundances which reflect the composition of the donor star, via the detection of strong emission and absorption resonance lines of C, N, O and Si (e.g. Nv 1240 Å, Civ 1549 Å, and Oi 1150, 1302 Å, (e.g. Gänsicke et al., 2003; Morales-Rueda et al., 2003; Sion et al., 2006)) which are not accessible in the optical. A single ultraviolet spectrum thus provides information on both the WD accretor and the donor star, offering a unique insight into the composition of the donor and the prior evolution of the system. A spectral fit to ultraviolet data also yields ac-

curate mass determinations, thus providing firm statistical constraints for the double-detonation scenario and the mass grow in CVs, finally confirming the potential of these systems as SN Ia progenitors. Finally, rotation rates of accreting WDs have been so far measured only in a handful of systems (e.g. Sion et al., 1994; Long et al., 2004). A resolving power of $\simeq 4000$ is sufficient to measure rotation rates $v \sin i \gtrsim 100$ km/s, thus providing robust observational constraints on the response of WDs to the accretion of mass and angular momentum.

3 Uniqueness

A wide-field, IFU-like instrument on board a space telescope optimized for UV observations ($\lambda = 90 - 350$ nm) will allow the community to simultaneously obtain photometric and spectroscopic observations with exquisite sensitivity in a wavelength regime that is not accessible from the ground, making it a unique instrument to tackle the scientific questions presented in Section 2. There are currently only two spectrographs on board *HST* that cover a wavelength range similar to the one that we propose (COS and STIS), one such spectrograph was launched on the stratospheric balloon FIREBall, and a new one is currently being proposed to be on board of the future LUVOIR telescope (LUMOS). In the following we discuss why these spectrographs are not suitable to achieve the science cases described in Section 2.

***HST*/COS**: the wavelength coverage of this spectrograph (λ = 90 - 320 nm) is similar to the one that we propose and it was designed to obtain spectroscopy of faint point-like sources (e.g. stars, quasars) with a resolving power R $\sim$ 1500 – 24000 (Green et al., 2012). The extremely small field of view of COS (2.5" diameter) however prevents observations of large patches of the sky and the possibility of observing extended objects, a critical requirement for all science cases presented in this document. Some of our science questions overlap with those that motivated COS, but the way we want to address them is substantially different. As an example, the question of whether the cosmic web exists and how baryons from galaxies interact with the surrounding medium can be tackled by COS by studying absorption spectra of intergalactic gas (e.g. Lyα forest, highly ionized absorption lines such as OIV, NV), whereas we propose to address this issue by studing the intergalactic medium in emission, through the detection of Lyα halos extended across hundreds of kpc (and possibly other rest-frame UV emission lines). Similarly, COS is suitable to study white dwarfs, cataclismic variables, and binary stars in the Milky Way. However the instrument that we propose will open up the new possibility to target these sources in globular clusters, dramatically increasing the statistics and efficiency of the observations.

***HST*/STIS**: this spectrograph and imaging camera covers the far- and near-UV wavelength range (λ = 115 – 310 nm, Woodgate et al. 1998). Spatially-resolved observations can be performed throught slitless spectroscopy, but the resolving power (R $\leq$ 2500) is too low to achieve our science goals (R $\gtrsim$ 4000 is needed). Furthermore the low throughtput of STIS ($\lesssim$ 10%) only allows observation of the brightest targets (the limiting magnitude V = 20.6 for an A0V star can be observed with a signal-to-noise ratio of 10 in 1 hour on source) and is not enough to reach the faint surface brightness levels required to achieve our goals (e.g. $SB_{Ly\alpha} \sim 10^{-19} - 10^{-20}$ erg s^{-1} cm^{-2} arcsec^{-2}, see Section 2.1).

FIREBall-2: this is a multi-object spectrograph operating in the UV and flying on a stratospheric balloon at an altitude of 40 km (Lemaitre et al., 2019). It follows the experiments started

with FIREBall-1 aimed at detecting the faint and diffuse emission of the intergalactic medium. It is equipped with a fiber IFU (300, 8" fibers). Part of the scientific motivation for FIREBall overlaps with the one proposed here (Section 2.1), but FIREBall only observes a limited wavelength range (200 - 210 nm) and targets the Lyα emission line at $z \sim 0.6 - 0.7$. We propose to cover a larger wavelength range ($\sim$ 90 – 350 nm), pushing the observations of Lyα up to z $\sim$ 1.7, starting to bridge the local and high-redshift Universe. Furthermore the field of view of FIREBall-2 is not contiguous (i.e. the fibers need to be placed in separate positions) and the spatial ($\sim$ 4") and spectral (R $\sim$ 2000) resolution are not enough to achieve our science goals. The overall throughtput of the instrument on FIREBall is $\sim$ 5% that is not enough to reach the low surface brightness level needed by our science goals. Finally, since this instrument works on a stratospheric balloon, its operations strongly depend on weather conditions and aeronautical rules. These kind of operational conditions cannot sustain a large demand from the astronomical community, but are key for testing new UV technologies.

***LUVOIR*/LUMOS**: this multi-object spectrograph covering the far-UV to visible wavelength range (λ = 100 – 1000 nm) is currently under study and is a candidate instrument for the future *LUVOIR* space mission (France et al., 2017). It will be able to observe hundreds of targets at once and will cover a field of view of 2' $\times$ 2'. However the field of view covered by LUMOS, as opposed to the IFU instrument that we are proposing, will not be contiguous. A 100% coverage of a large field of view to a high depth is critical to efficiently achieve our science goals, such as contiguously map the extended emission of the cosmic web and galaxy halos, the extended tidal tails around galaxy cluster members, globular clusters that host populations of accreting white dwarfs. A discontiguous field of view drastically reduces the efficiency of the observations and the discovery potential. Additionally, compared to a multi-object spectrograph that can only perform pointed observations, the IFU instrument that we propose will provide thousands of spectra with a single pointing and will therefore have a unique potential for serendipitous discoveries. Finally, LUMOS is designed to observe at the diffraction limit, a condition that would prevent us from achieving the extremely low surface brightness levels needed by our science cases.

4 Synergies

In the next two decades all the major facilities are expected to operate at red and IR wavelengths (e.g. *JWST*, ELT). A window on the UV will therefore offer a complementary view at shorter wavelengths and will have strong synergies with these facilities. It will be critical to conduct follow-up observations in the UV regime, in an epoch when *HST* will not be operational anymore. An IFU-like instrument operating in the UV will also provide targets that can then be followed-up with the ELT (e.g. the gas stripped from galaxy cluster members observed in Lyα can be observed in [OII] and Hα with ELT/HARMONI providing information on the ionized gas). Furthermore most of the science questions presented here have synergies with future major facilities such as SKA at longer wavelengths (e.g. to detect the HI gas stripped in cluster members and the cosmic web around galaxies) and will benefit from targets identified by *Euclid* and LSST in large field imaging. There are also synergies with ALMA, should it still be operational (e.g. the gas stripped by cluster members might be detected both in the neutral phase

Table 1: Main (range of) parameters of the telescope and instrument.

Focal length	20 - 30 m
Aperture	0.9 - 1.1 m
F-number	F/10 - F/25
Field of view	1×1 arcmin^2
Wavelength range	90 – 350 nm (preferred) 100 – 300 nm (minimum requirement)
Spectral resolution	average R = 4000
Spectral sampling	0.5 Å per spectral bin
Spatial sampling	0.5" × 1" per spaxel
Spatial resolution (FWHM)	2" – 3"
Throughtput	$\gtrsim 25\%$ over the whole wavelength range

through Lyα emission with our proposed instrument and in the molecular phase with ALMA). Finally synergies with *Athena* and *LISA* will enhance the discovery potential (e.g. *Athena* will unveil the hot gas phase stripped by cluster members and visible in the X-rays, while *LISA* will detect the gravitational waves produced by the most compact accreting white dwarfs with short orbital periods).

5 Technical concept

In this section we present some key design parameters for a system compliant with the proposed science theme. We notice that a dedicated space mission is not strictly required and an instrument hosted on another future spacecraft is sufficient. Finally, we highlight that a system study has not been performed, as this goes beyond the scope of the proposal.

Given the main characteristics of the telescope (Table 1), the dedicated space mission will be an M-size one.

A UV integral field unit (IFU) will be required to achieve the science goals presented in this proposal. Part of the technology that has already been developed for the ground-based Multi Unit Spectroscopic Explorer (MUSE) on the Very Large Telescope (VLT) and that is currently being designed for BlueMUSE (extending towards bluer wavelengths λ = 350 – 600 nm) can be adapted for this project. Insights on the performances of IFUs in space can also be obtained from *JWST*/NIRSpec, when launched (although NIRSpec will operate at IR wavelengths). Such an instrument will extend the capabilities of IFUs toward bluer wavelengths, λ = 90 – 350 nm, not observable from the ground, targeting different science cases. It will have a single instrumental setup (i.e. fixed spectral and spatial setup), which simplifies the overall fore-optics. A rapid response mode will be needed to carry out observations of transients (Section 2.4). We summarize in Table 1 the main characteristics of the instrument.

Due to the complexity and extent of the optics, IFUs tend to be heavy instruments, an important constraint for a space mission. The mass of this instrument will be one of the main design drives.

The thermal environment is also one of the main design drivers for optics in space. It would be preferable to perform the proposed observations above 260 K to prevent absorption on reflective surfaces, given that UV systems are sensitive even to mono-layers of contaminants (LUVOIR, 2018). An operating temperature in the range 270 K – 290 K assures better performances and will facilitate mission development because testing, alignment, and mirrors polishing and figuring can be performed on the ground without cryogenic facilities, with a smaller number of iterations and eventually reduced complexity. Besides, launch shocks are an important design constraint and are far more critical at cold. The detectors are an exception to the above mentioned temperature range, as cryogenic temperatures are likely required to maximize their performance.

In line with decades of warm optics design, the traditional choices for the material of the mirrors are Zerodur™ and ULE™ thanks to their high stability. Silicon Carbide (SiC) is also an option, as detailed below.

A sun-synchronous orbit would be preferable for this mission to avoid eclipses and operate in a more stable environment. However, this is not a strict constraint and UV observations have extensively been performed by other telescopes (e.g. *HST*) on different orbits.

Finally, a significant amount of data will be produced during the observations. This will require an appropriate design of on-board computers and transmission.

5.1 Technological challenges

The development of a UV-optimized mission as the one proposed here will pose several technological challenges and in turn will offer the possibility to advance in many areas such as material science, detector technology, lightweight active optics, thermal control, space mechanisms, precision guidance and navigation, and data transmission and analysis.

First of all, space-based instruments that are currently operational at UV wavelengths have a throughtput $< 25\%$ in the wavelength range $\lambda = 200 - 400$ nm (e.g. WFC3 UVIS filters on board *HST*). To achieve our goals a throughtput $\gtrsim 25\%$ is needed. Such performance is currently hindered by the decrement of reflectivity below 110 nm. Aluminium has in principle a good reflectivity down to wavelengths of ~ 100 nm, but it has the known tendency to oxidation, so the actual performances are comparable to those of other typical mirror coatings (e.g. silver and gold). However there are already promising studies on this subject (Balasubramanian et al. 2017, Del Hoyo & Quijada 2017) that point to the use of protective layers to prevent aluminum oxidation from degrading the performance. A high reflectivity surface below 110 nm is therefore a reasonable technological advancement foreseen for the near future.

UV detector technology will be pushed as well by a mission covering the science theme of this proposal. In particular, to achieve the proposed science goals we need to reach very low surface brightness levels. As an example, to detect the Lyα emission from the circumgalactic medium we need to reach a surface brightness $\mathrm{SB}_{\mathrm{Ly}\alpha} \sim 10^{-19}\,\mathrm{erg\,s^{-1}\,cm^{-2}\,arcsec^{-2}}$. Given the characteristics of the proposed telescope and instrument (Table 1), this translates in a detection threshold of $\sim 0.2 - 1\ \mathrm{e^-\ pixel^{-1}\ hr^{-1}}$. Currently the main limitation to reach such low detection thresholds is given by the read out noise of the detectors ($\sim 2 - 3\ \mathrm{e^-}$ for both CMOS and CCDs). However, there are ongoing studies focusing on enhancing UV detector performances and reducing the read out noise (e.g. EMCCDs that use avalanche gain on the readout). This new

technology is tested in sub-orbital flights on FIREBall (Hamden et al. 2016, 2019). Other recent studies are proposing to develop a CMOS detector with readout noise below 0.1 e^-, such that single photons would be detectable (link). Additionally, 8k $\times$ 8k devices exist already, although they are not optimized yet for the UV and they still have a relatively high readout noise.

An alternative to traditional detectors is the use of a "spectrometer on a chip" (i.e. every photon that hits the detector has a measured energy) based on MKID technology. This kind of spectrometers are already in use for DARKNESS (Meeker et al., 2018) and have no dark current or readout noise in the traditional sense, as they measure thousands to millions of quasiparticles for every photon that hits. However, they are subject to quasiparticles fluctuations, limiting the precision with which the energy of the photons can be measured and in turn the achievable spectral resolution. In fact, the spectral resolution that they can currently achieve is only $R < 100$, but theoretically it could be much higher and there is already interest toward using these technology in space (Rauscher et al., 2016). Another limitation is that MKIDs today require a superconducting layer and therefore extreme cryogenic temperatures ($\approx$1 K).

Regardless of the cryogenic environment and superconductivity, which are alone areas of development, thermal control in the order of 10^{-2} K is a challenge, especially if non-conventional materials are employed.

Using SiC as mirror substrate is a serious option to be considered. In fact, while it poses some challenges on the surface finishing and requires more stringent constraints on the thermal control, it has significant advantages in terms of controllability thanks to its superior strength. A set of actuators (e.g. piezo-stacks) annealed in the SiC substrate, allows compensating wavefront errors in several load conditions, including on-ground testing in 1-g. Thin active mirrors are also an interesting and promising approach, although not yet mature.

Finally, dedicated precision mechanisms on the optics or micronewton thrusters, following the heritage of GAIA and LISA-Pathfinder (Armano et al., 2019), are very promising solutions (Dennehy & Alvarez-Salazar, 2018) to avoid the need for devices that produce unacceptable vibrations while observing, such as the reaction wheels.

6 Conclusions

An entire new window on the Universe is opened by exploring its UV-range with high spatial and spectral resolution. We have showcased several different science questions to be addressed in the time frame of Voyage 2050, and highlighted how our approach will ensure ample opportunities for serendipitous discoveries.

The ideal instrument to answer the proposed scientific questions is a UV-optimized, wide-field IFU. It could be hosted by a future telescope or alternatively by a new M-size mission and it will be the only UV IFU in space. Designing and building such a complex system will encourage the technological development of several areas, including material science, data acquisition and reduction, UV detector technology, and micro-vibrations mitigation.

Finally, by focusing on the UV wavelength range after and during an epoch when the largest available facilities have been operating at red and IR wavelengths (e.g. *JWST*, ELT), this instrument will open up a new discovery space and will be suitable to work in synergy with the main available observatories now in development such as *Athena*, the ELT and SKA.

References

Aravena, M., Carilli, C. L., Salvato, M., et al. 2012, MNRAS, 426, 258

Armano, M., Audley, H., Baird, J., et al. 2019, Phys. Rev. D, 99, 122003

Arrigoni Battaia, F., Hennawi, J. F., Cantalupo, S., & Prochaska, J. X. 2016, ApJ, 829, 3

Arrigoni Battaia, F., Hennawi, J. F., Prochaska, J. X., et al. 2019, MNRAS, 482, 3162

Arrigoni Battaia, F., Prochaska, J. X., Hennawi, J. F., et al. 2018, MNRAS, 473, 3907

Augustin, R., Péroux, C., Møller, P., et al. 2018, MNRAS, 478, 3120

Bacon, R., Accardo, M., Adjali, L., et al. 2010, 7735, doi:10.1117/12.856027

Balasubramanian, K., Hennessy, J., Raouf, N., et al. 2017, 10398, 103980X

Bell, E. F., McIntosh, D. H., Barden, M., et al. 2004, ApJL, 600, L11

Bersten, M. C., Benvenuto, O. G., Nomoto, K., et al. 2012, ApJ, 757, 31

Bertone, S., & Schaye, J. 2012, MNRAS, 419, 780

Bildsten, L., Shen, K. J., Weinberg, N. N., & Nelemans, G. 2007, ApJL, 662, L95

Bildsten, L., Townsley, D. M., Deloye, C. J., & Nelemans, G. 2006, ApJ, 640, 466

Blanton, M. R., & Moustakas, J. 2009, ARA&A, 47, 159

Bond, J. R., Kofman, L., & Pogosyan, D. 1996, Nature, 380, 603

Borisova, E., Cantalupo, S., Lilly, S. J., et al. 2016, ApJ, 831, 39

Boselli, A., Boissier, S., Cortese, L., et al. 2006, ApJ, 651, 811

Boselli, A., & Gavazzi, G. 2014, A&AR, 22, 74

Branch, D., & Tammann, G. A. 1992, ARA&A, 30, 359

Burrows, A. 2013, Rev. Mod. Phys., 85, 245

Cai, Z., Fan, X., Yang, Y., et al. 2017, ApJ, 837, 71

Cai, Z., Hamden, E., Matuszewski, M., et al. 2018, ApJL, 861, L3

Cantalupo, S., Arrigoni-Battaia, F., Prochaska, J. X., Hennawi, J. F., & Madau, P. 2014, Nature, 506, 63

Cantalupo, S., Porciani, C., Lilly, S. J., & Miniati, F. 2005, ApJ, 628, 61

Christensen, L., Jahnke, K., Wisotzki, L., & Sánchez, S. F. 2006, A&A, 459, 717

Cimatti, A., Cassata, P., Pozzetti, L., et al. 2008, A&A, 482, 21

Coogan, R. T., Daddi, E., Sargent, M. T., et al. 2018, MNRAS, 479, 703

Croton, D. J., Springel, V., White, S. D. M., et al. 2006, MNRAS, 365, 11

Daddi, E., Dickinson, M., Morrison, G., et al. 2007, ApJ, 670, 156

Dannerbauer, H., Lehnert, M. D., Emonts, B., et al. 2017, A&A, 608, A48

Dekel, A., & Birnboim, Y. 2006, MNRAS, 368, 2

Del Hoyo, J., & Quijada, M. 2017, doi:10.1117/12.2274399

Dennehy, C., & Alvarez-Salazar, O. S. 2018, Spacecraft Micro-Vibration: A Survey of Problems, Experiences, Potential Solutions, and Some Lessons Learned, Tech. Rep. NASA/TM-2018-220075, NASA

Dressler, A. 1980, ApJ, 236, 351

Farina, E. P., Venemans, B. P., Decarli, R., et al. 2017, ApJ, 848, 78

Fink, M., Röpke, F. K., Hillebrandt, W., et al. 2010, A&A, 514, A53

Fossati, M., Fumagalli, M., Boselli, A., et al. 2016, MNRAS, 455, 2028

France, K., Fleming, B., West, G., et al. 2017, in Society of Photo-Optical Instrumentation Engineers (SPIE) Conference Series, Vol. 10397, Proc. SPIE, 1039713

Fumagalli, M., Fossati, M., Hau, G. K. T., et al. 2014, MNRAS, 445, 4335

Fumagalli, M., Krumholz, M. R., Prochaska, J. X., Gavazzi, G., & Boselli, A. 2009, ApJ, 697, 1811

Gal-Yam, A., Arcavi, I., Ofek, E. O., et al. 2014, Nature, 509, 471

Gallego, S. G., Cantalupo, S., Lilly, S., et al. 2018, MNRAS, 475, 3854

Gänsicke, B. T., Long, K. S., Barstow, M. A., & Hubeny, I. 2006, ApJ, 639, 1039

Gänsicke, B. T., Szkody, P., de Martino, D., et al. 2003, ApJ, 594, 443

Gavazzi, G., & Jaffe, W. 1985, ApJL, 294, L89

Gould, A., & Weinberg, D. H. 1996, ApJ, 468, 462

Green, J. C., Froning, C. S., Osterman, S., et al. 2012, ApJ, 744, 60

Groh, J. H. 2014, A&A, 572, L11

Gunn, J. E., & Gott, J. Richard, I. 1972, ApJ, 176, 1

Haardt, F., & Madau, P. 2012, ApJ, 746, 125

Haiman, Z., & Rees, M. J. 2001, ApJ, 556, 87

Hamden, E. T., Jewell, A. D., Shapiro, C. A., et al. 2016, Journal of Astronomical Telescopes, Instruments, and Systems, 2, 036003

Hamden, E. T., Hoadley, K., Martin, D. C., et al. 2019, arXiv e-prints, arXiv:1905.00433

Haynes, M. P. 1985, in European Southern Observatory Conference and Workshop Proceedings, Vol. 20, 45–50

Heckman, T. M., Miley, G. K., Lehnert, M. D., & van Breugel, W. 1991, ApJ, 370, 78

Hennawi, J. F., Prochaska, J. X., Cantalupo, S., & Arrigoni-Battaia, F. 2015, Science, 348, 779

Hopkins, P. F., Kereš, D., Murray, N., Quataert, E., & Hernquist, L. 2012, MNRAS, 427, 968

Hu, E. M., & Cowie, L. L. 1987, ApJL, 317, L7

Husser, T.-O., Kamann, S., Dreizler, S., et al. 2016, A&A, 588, A148

Ivanova, N., Heinke, C. O., Rasio, F. A., et al. 2006, MNRAS, 372, 1043

Johansson, P. H., Burkert, A., & Naab, T. 2009, ApJL, 707, L184

Kennicutt, Jr., R. C. 1998, ApJ, 498, 541

Khazov, D., Yaron, O., Gal-Yam, A., et al. 2016, ApJ, 818, 3

Knigge, C. 2012, 83, 549

Kollmeier, J. A., Zheng, Z., Davé, R., et al. 2010, ApJ, 708, 1048

Krogager, J. K., Møller, P., Fynbo, J. P. U., & Noterdaeme, P. 2017, MNRAS, 469, 2959

Kupfer, T., Korol, V., Shah, S., et al. 2018, MNRAS, 480, 302

Larson, R. B., Tinsley, B. M., & Caldwell, C. N. 1980, ApJ, 237, 692

Lemaitre, G., Grange, R., Quiret, S., et al. 2019, arXiv e-prints, arXiv:1903.02218

Li, W., Chornock, R., Leaman, J., et al. 2011, MNRAS, 412, 1473

Long, K. S., Sion, E. M., Gänsicke, B. T., & Szkody, P. 2004, ApJ, 602, 948

Lusso, E., Fumagalli, M., Fossati, M., et al. 2019, MNRAS, 485, L62

LUVOIR. 2018, arXiv e-prints, arXiv:1809.09668

Madau, P., & Dickinson, M. 2014, ARA&A, 52, 415

Martig, M., Bournaud, F., Teyssier, R., & Dekel, A. 2009, ApJ, 707, 250

Martin, D. C., Chang, D., Matuszewski, M., et al. 2014, ApJ, 786, 106

Maund, J. R., Fraser, M., Ergon, M., et al. 2011, ApJ, 739, L37

Meeker, S. R., Mazin, B. A., Walter, A. B., et al. 2018, PASP, 130, 065001

Meiksin, A. A. 2009, Reviews of Modern Physics, 81, 1405

Møller, P., Warren, S. J., Fall, S. M., Jakobsen, P., & Fynbo, J. U. 2000, The Messenger, 99, 33

Morales-Rueda, L., Marsh, T. R., Steeghs, D., et al. 2003, A&A, 405, 249

Morrissey, P., Matuszewski, M., Martin, C., et al. 2012, 8446, 844613

Nakar, E., & Sari, R. 2010, ApJ, 725, 904

Nelemans, G., Yungelson, L. R., van der Sluys, M. V., & Tout, C. A. 2010, MNRAS, 401, 1347

Noterdaeme, P., Petitjean, P., Carithers, W. C., et al. 2012, A&A, 547, L1

Pala, A. F., Gänsicke, B. T., Townsley, D., et al. 2017, MNRAS, 466, 2855

Peng, Y., Maiolino, R., & Cochrane, R. 2015, Nature, 521, 192

Peng, Y.-j., Lilly, S. J., Kovač, K., et al. 2010, ApJ, 721, 193

Perlmutter, S., Aldering, G., Goldhaber, G., et al. 1999, ApJ, 517, 565

Pieri, M. M., Mortonson, M. J., Frank, S., et al. 2014, MNRAS, 441, 1718

Quiret, S., Péroux, C., Zafar, T., et al. 2016, MNRAS, 458, 4074

Rabinak, I., & Waxman, E. 2011, ApJ, 728, 63

Rahmani, H., Péroux, C., Turnshek, D. A., et al. 2016, MNRAS, 463, 980

Rauscher, B. J., Canavan, E. R., Moseley, S. H., Sadleir, J. E., & Stevenson, T. 2016, Journal of Astronomical Telescopes, Instruments, and Systems, 2, 041212

Rees, M. J. 1988, MNRAS, 231, 91p

Riess, A. G., Filippenko, A. V., Challis, P., et al. 1998, AJ, 116, 1009

Rubin, A., & Gal-Yam, A. 2017, ApJ, 848, 8

Sanders, D. B., & Mirabel, I. F. 1996, ARA&A, 34, 749

Sapir, N., & Waxman, E. 2017, ApJ, 838, 130

Scarlata, C., Colbert, J., Teplitz, H. I., et al. 2009, ApJL, 704, L98

Schmidt, M. 1959, ApJ, 129, 243

Shull, J. M., Danforth, C. W., & Tilton, E. M. 2014, ApJ, 796, 49

Sion, E. M. 1995, ApJ, 438, 876

Sion, E. M., Gänsicke, B. T., Long, K. S., et al. 2008, ApJ, 681, 543

Sion, E. M., Long, K. S., Szkody, P., & Huang, M. 1994, ApJL, 430, L53

Sion, E. M., Solheim, J.-E., Szkody, P., Gaensicke, B. T., & Howell, S. B. 2006, ApJL, 636, L125

Smartt, S. J. 2015, PASA, 32, e016

Smartt, S. J., Eldridge, J. J., Crockett, R. M., & Maund, J. R. 2009, MNRAS, 395, 1409

Smartt, S. J., Maund, J. R., Hendry, M. A., et al. 2004, Sci, 303, 499

Speagle, J. S., Steinhardt, C. L., Capak, P. L., & Silverman, J. D. 2014, ApJS, 214, 15

Steidel, C. C., Erb, D. K., Shapley, A. E., et al. 2010, ApJ, 717, 289

Szkody, P., Anderson, S., Agüeros, M., & Covarrubias, R. 2002, in Astronomical Society of the Pacific Conference Series, Vol. 261, The Physics of Cataclysmic Variables and Related Objects, ed. B. T. Gänsicke, K. Beuermann, & K. Reinsch, 297

Toft, S., Smolčić, V., Magnelli, B., et al. 2014, ApJ, 782, 68

Toloba, E., Boselli, A., Cenarro, A. J., et al. 2011, A&A, 526, A114

Townsley, D. M., & Bildsten, L. 2003, ApJL, 596, L227

—. 2004, ApJ, 600, 390

Townsley, D. M., & Gänsicke, B. T. 2009, ApJ, 693, 1007

Tumlinson, J., Peeples, M. S., & Werk, J. K. 2017, ARA&A, 55, 389

Van Dyk, S. D. 2017, in Handbook of Supernovae, ed. A. W. Alsabti & P. Murdin (Cham: Springer International Publishing), 693–719

Waxman, E., Mészáros, P., & Campana, S. 2007, ApJ, 667, 351

Weidinger, M., Møller, P., & Fynbo, J. P. U. 2004, Nature, 430, 999

Weidinger, M., Møller, P., Fynbo, J. P. U., & Thomsen, B. 2005, A&A, 436, 825

White, S. D. M., Frenk, C. S., Davis, M., & Efstathiou, G. 1987, ApJ, 313, 505

Wisotzki, L., Bacon, R., Brinchmann, J., et al. 2018, Nature, 562, 229

Witstok, J., Puchwein, E., Kulkarni, G., Smit, R., & Haehnelt, M. G. 2019, arXiv e-prints, arXiv:1905.06954

Woodgate, B. E., Kimble, R. A., Bowers, C. W., et al. 1998, PASP, 110, 1183

Yaron, O., Perley, D. A., Gal-Yam, A., et al. 2017, NatPh, 13, 510